This article has been accepted for publication in a future issue of this journal, but has not been fully edited. Content may change prior to final publication. Citation information: DOI 10.1109/TVT.2013.2293580, IEEE Transactions on Vehicular Technology

A Tractable Framework for Exact Probability of Node Isolation and Minimum Node Degree Distribution in Finite Multi-hop Networks

Zubair Khalid, *Member, IEEE*, Salman Durrani, *Senior Member, IEEE* and Jing Guo, *Student Member, IEEE*

***Abstract*—This paper presents a tractable analytical framework for the exact calculation of the probability of node isolation and the minimum node degree distribution when N sensor nodes are independently and uniformly distributed inside a finite square region. The proposed framework can accurately account for the boundary effects by partitioning the square into subregions, based on the transmission range and the node location. We show that for each subregion, the probability that a random node falls inside a disk centered at an arbitrary node located in that subregion can be expressed analytically in closed-form. Using the results for the different subregions, we obtain the exact probability of node isolation and minimum node degree distribution that serves as an upper bound for the probability of k-connectivity. Our theoretical framework is validated by comparison with the simulation results and shows that the minimum node degree distribution serves as a tight upper bound for probability of k-connectivity. The proposed framework provides a very useful tool to accurately account for the boundary effects in the design of finite wireless networks.**

***Index Terms*—Wireless multi-hop networks, sensor networks, probability of node isolation, node degree distribution, probability of connectivity, k-connectivity.**

I. Introduction

Wireless multi-hop networks, also refereed to as wireless sensor networks and wireless ad hoc networks, consist of a group of sensor nodes deployed over a finite region [1]–[5]. The nodes operate in a decentralized manner without the need of any fixed infrastructure, i.e., the nodes communicate with each other via a single-hop wireless path (if they are in range) or via a multi-hop wireless path. In most of the applications, such wireless networks are formed by distributing a finite (small) number of nodes in a finite area, which is typically assumed to be a square region [6]–[9].

Connectivity is a basic requirement for the planning and effective operation of wireless multi-hop networks [10], [11]. The k-connectivity is a most general notion of connectivity and an important characteristic of wireless multi-hop networks [9], [12], [13]. The network being k-connected ensures that there exists at least k *independent* multi-hop paths between any two nodes. In other words, k-connected network would still be 1-connected if $(k-1)$ nodes forming the network fail. The *probability of node isolation*, defined as the probability that a randomly selected node has no connections to any other nodes, plays a key role in determining the overall network connectivity (1-connectivity) [12], [14]. The *minimum node degree distribution*, which is the probability that each node in the network has at least k neighbours, is crucial in determining the k-connectivity of the network [12].

For large-scale wireless sensor networks, assuming Poisson distributed nodes in an infinite area, the connectivity properties such as probability of isolation, average node degree, k-connectivity have been well studied [12], [15]–[21]. When the node locations follow an infinite homogeneous Poisson point process and assuming all nodes have the same transmission range, it has been shown that the network becomes k-connected with high probability (close to 1) at the same time the minimum node degree of the network approaches k [15]. This fact was used to approximate the probability of k-connectivity by the minimum node degree distribution in [12]. It was also used to determine the asymptotic value of the minimum transmission range for k-connectivity for a uniform distribution of nodes in a unit square and disk [9].

A. Related Work

Since many practical multi-hop networks are formed by distributing a finite number of nodes in a finite area, there has been an increasing interest to model and determine the connectivity properties in finite multi-hop networks [9], [12], [14], [22]–[27]. This is also due to the fact, established earlier in [12], [14] and recently in [25], that the asymptotic connectivity results for large-scale networks provide an extremely poor approximation for finite wireless networks. This poor approximation is due to the boundary effects experienced by the nodes near the borders of the finite region over which the nodes are deployed. Since the nodes located close to the physical boundaries of the network have a limited coverage area, they have a greater probability of isolation. Therefore, the boundary effects play an important role in determining the overall network connectivity.

Different approaches have been used in the literature, to try to model the boundary effects including (i) using geometrical probability [28] and dividing the square region into smaller subregions to facilitate asymptotic analysis of the transmission range for k-connectivity [9], [22] and to find mean node degree in different subregions [29], (ii) using a cluster expansion approach and decomposing the boundary effects into corners and

The authors are with the Research School of Engineering, College of Engineering and Computer Science, The Australian National University, Canberra, ACT 0200, Australia. Emails: {zubair.khalid, salman.durrani, jing.guo}@anu.edu.au

This article has been accepted for publication in a future issue of this journal, but has not been fully edited. Content may change prior to final publication. Citation information: DOI 10.1109/TVT.2013.2293580, IEEE Transactions on Vehicular Technology

edges to yield high density approximations [27] and (iii) using a deterministic grid deployment of nodes in a finite area [30] to approximate the boundary effects with random deployment of nodes [25]. The above approaches provide bounds, rather than exact results, for the probability of node isolation and/or probability of connectivity. For a wireless network deployed over a finite area, the existing results for k-connectivity and minimum node degree are asymptotic (infinite N) [9], [31]. An attempt was made in [17] to study the minimum node degree and k-connectivity by circumventing modeling of the boundary effects but the results were shown to be valid for large density (number of nodes) only. Therefore, it is still largely an open research problem to characterize the boundary effects and to find general frameworks for deriving the exact results for the probability of node isolation and the minimum node degree distribution, when a finite number of nodes are independently and uniformly distributed inside a finite region.

B. Contributions

In the above context, we address the following open questions in this paper for a wireless network of N nodes, which are uniformly distributed over a square region:

Q1 How can we accurately account for the boundary effects to determine the exact probability of node isolation?

Q2 How can we incorporate the boundary effects to find the minimum node degree distribution?

In this paper, addressing the above two open questions, we present a tractable analytical framework for the exact calculation of the probability of node isolation and the minimum node degree distribution in finite wireless multi-hop networks, when N nodes are independently and uniformly distributed in a square region. Our proposed framework partitions the square into unequal subregions, based on the transmission range and the location of an arbitrary node. Using geometrical probability, we show that for each subregion, the probability that a random node falls inside a disk centered at an arbitrary node located in that subregion can be expressed analytically in closed-form. This framework accurately models the boundary effects and leads to an exact expression for the probability of node isolation and the minimum node degree distribution, which can be easily evaluated numerically. We show that the minimum node degree distribution can be used as an upper bound for the probability of k-connectivity.

Since the k-connectivity depends on the number of nodes deployed over the finite region and the transmission range of each node [9], [31], the transmission range must be large enough to ensure that the network is connected but small enough to minimize the power consumption at each node and interference between nodes [12], [32], which in turn maximizes the network capacity. This fundamental trade-off between the network connectivity and the network capacity leads to the following network design question:

Q3 Given a network of N nodes distributed over a square region, what is the minimum transmission range such that a network is connected with a high probability or alternatively, what is the minimum number of nodes for a given transmission range such that the network is connected?

Addressing this network design problem, we show through an example how the proposed framework can be used to determine the minimum transmission range required for the network to be connected with high probability.

The rest of the paper is organized as follows. The system model, problem formulation and connectivity properties of a wireless network are presented in Section II. The proposed framework to evaluate the probability of node isolation and the minimum node degree distribution is provided in Section III. The boundary effects in the different regions formed with the change in transmission range are presented in Section IV. The validation of the proposed framework via simulation results and the design example are presented in Section V. Finally, Section VI concludes the paper.

II. System Model and Problem Formulation

A. Distribution of Nodes and Node Transmission Model

Consider N nodes which are uniformly and independently distributed inside a square region $\mathcal{R} \in \mathbb{R}^2$, where $\mathbb{R}^2$ denotes the two dimensional Euclidean domain. Let S_ℓ and V_ℓ, for $\ell \in \{1,2,3,4\}$, denote the side and vertex of the square, respectively, which are numbered in an anticlockwise direction. Without loss of generality, we assume that the first vertex V_1 of the square is located at the origin $(0,0)$ and we consider a unit square region defined as

$$\mathcal{R} = \{\boldsymbol{u} = (x,y) \in \mathbb{R}^2 | \, 0 \leq x \leq 1, \, 0 \leq y \leq 1\}. \quad (1)$$

Let $\boldsymbol{u} = (x,y)$ denote the position of an arbitrary node inside the square $\mathcal{R}$. The node distribution probability density function (PDF) can be expressed as

$$f_{\mathbf{U}}(\boldsymbol{u}) = \begin{cases} 1 & \boldsymbol{u} \in \mathcal{R}, \\ 0 & \boldsymbol{u} \in \mathbb{R}^2 \backslash \mathcal{R}. \end{cases} \quad (2)$$

We define $|\mathcal{R}| = \int_{\mathcal{R}} ds(\boldsymbol{u})$ as a measure of the physical area of the square region, where $ds(\boldsymbol{u}) = dxdy$ and the integration is performed over the two dimensional square region $\mathcal{R}$. Note that $|\mathcal{R}| = 1$ since we assume a unit square.

We assume that each sensor node has a fixed transmission range r_{o} and the *coverage region* of a node located at $\boldsymbol{u}$ is then a disk $\mathcal{O}(\boldsymbol{u}; r_{\mathrm{o}})$ of radius r_{o} centered at the node. Note that the *coverage area* $|\mathcal{O}(\boldsymbol{u}; r_{\mathrm{o}})| = \pi r_{\mathrm{o}}^2$. The number of nodes inside the coverage area of a certain node are termed as its neighbors.

B. Connectivity Properties

In this subsection, we define the key connectivity properties of a multi-hop network, which are considered in this paper.

Definition 1 (Conditional Probability of Connectivity): Let the cumulative distribution function (CDF) $F(\boldsymbol{u}; r_{\mathrm{o}})$ denote the conditional probability of connectivity that a randomly placed node according to uniform probability density function (PDF) is connected to a node located at $\boldsymbol{u}$. Mathematically,

$$F(\boldsymbol{u}; r_{\mathrm{o}}) \triangleq |\mathcal{O}(\boldsymbol{u}; r_{\mathrm{o}}) \cap \mathcal{R}|. \quad (3)$$

This article has been accepted for publication in a future issue of this journal, but has not been fully edited. Content may change prior to final publication. Citation information: DOI 10.1109/TVT.2013.2293580, IEEE Transactions on Vehicular Technology

Definition 2 (Probability of Node Isolation): Let $P_{\text{iso}}(r_{\text{o}})$ denote the probability of node isolation that any node in the network is isolated. Assuming that the probability of node isolation is independent for each node, the probability that a given node at $\boldsymbol{u}$ is isolated is given by $(1 - F(\boldsymbol{u}; r_{\text{o}}))^{N-1}$, which can be averaged over all possible locations to evaluate $P_{\text{iso}}(r_{\text{o}})$ as

$$P_{\text{iso}}(r_{\text{o}}) \triangleq \int_{\mathbb{R}^2} (1 - F(\boldsymbol{u}; r_{\text{o}}))^{N-1} f_{\mathbf{U}}(\boldsymbol{u}) ds(\boldsymbol{u}) = \int_{\mathcal{R}} (1 - F(\boldsymbol{u}; r_{\text{o}}))^{N-1} ds(\boldsymbol{u}). \quad (4)$$

Definition 3 (Minimum Node Degree): For a uniform distribution of N nodes in a square region, define the minimum node degree as the minimum of number of neighbors of *any* node in the region. Let the discrete random variable D denote the minimum node degree. The associated PDF, termed as the minimum node degree distribution is given by

$$f_D(k; r_{\text{o}}) = \text{P}(D = k) \triangleq \left(1 - \sum_{d=0}^{k-1} \binom{N-1}{d} \times \int_{\mathcal{R}} (F(\boldsymbol{u}; r_{\text{o}}))^d (1 - F(\boldsymbol{u}; r_{\text{o}}))^{N-d-1} ds(\boldsymbol{u})\right)^N. \quad (5)$$

The details of the formulation of $f_D(k; r_{\text{o}})$ are provided in Appendix A.

Definition 4 (1-connected network): A network of N nodes is said to be 1-connected (or connected) if there exists at least one path between any pair of randomly chosen nodes.

Definition 5 (k-connected network): A network of N nodes is said to be k-connected ($k = 1, 2, \ldots, N-1$) if there exist at least k mutually independent paths between any pair of randomly chosen nodes. In other words, a network is k-connected if the network stays 1-connected with the removal of any $(k-1)$ nodes. Let $P_{\text{k-con}}(r_{\text{o}})$ denote the probability that the network of N nodes (each with transmission range r_{o}) is k-connected.

Next we examine the relation between probability $P_{\text{k-con}}(r_{\text{o}})$ and the minimum node degree distribution $f_D(k; r_{\text{o}})$. Penrose [15] presented in his work on graph theory that a random network for large enough number of nodes, becomes k-connected at the same instant it acheives the minimum node degree k with high probability, that is, $f_D(k; r_{\text{o}})$ serves as an upper bound on $P_{\text{k-con}}(r_{\text{o}})$, which gets tighter as both $f_D(k; r_{\text{o}})$ and $P_{\text{k-con}}(r_{\text{o}})$ approach one or the number of nodes approaches infinity. Mathematically, we can express this as

$$f_D(k; r_{\text{o}}) \geq P_{\text{k-con}}(r_{\text{o}}), \quad f_D(k; r_{\text{o}}) = P_{\text{k-con}}(r_{\text{o}}), \quad P_{\text{k-con}}(r_{\text{o}}) \to 1. \quad (6)$$

We note that the minimum node degree distribution is of fundamental importance [12] as (i) it determines the connectivity of the network ($P_{\text{1-con}}(r_{\text{o}})$), (ii) takes into account the failure of the nodes and (iii) also determines the minimum node degree of the network ($P_{\text{k-con}}(r_{\text{o}})$). Using (4) and (5), we also note the relationship between $P_{\text{iso}}(r_{\text{o}})$ and $f_D(k; r_{\text{o}})$:

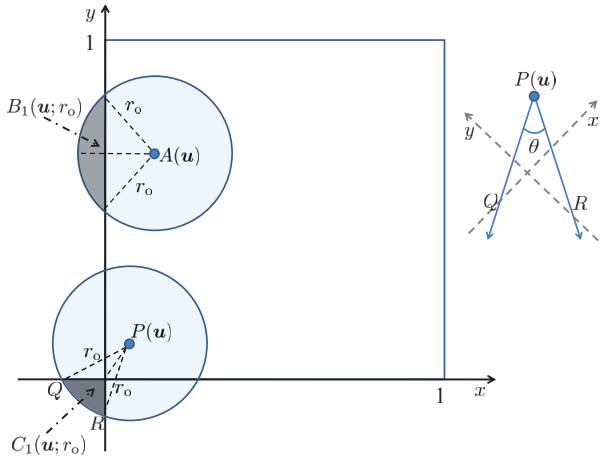

Fig. 1: Illustration of border and corner effects in a unit square.

$f_D(1; r_{\text{o}}) = (1 - P_{\text{iso}}(r_{\text{o}}))^N$. Since $f_D(1; r_{\text{o}})$ denotes the probability that each node has at least one neighbor, it has been also referred to as the probability of no isolated node in the literature [12], [14].

C. Problem Statement

There are two key challenges in evaluating the probability of node isolation $P_{\text{iso}}(r_{\text{o}})$ in (4) and the minimum node degree distribution $f_D(k; r_{\text{o}})$ in (5). The *first challenge* is to find the CDF in (3), which requires the evaluation of the overlap area $|\mathcal{O}(\boldsymbol{u}; r_{\text{o}}) \cap \mathcal{R}|$. In [23], it is proposed to find this intersection area using polar coordinates and dividing the square into different radial regions. However, due to the dependance between the polar radius and the polar angle, this approach does not lead to closed-form solutions. In [33], an alternative approach is presented for finding the intersection area by first finding the area of circular segments formed outside the sides and vertices and then subtracting from the area of the disk. This approach leads to closed-form solutions and is adopted in this work.

The *second challenge* is to average the CDF given in (3) over the square in order to determine the probability of node isolation $P_{\text{iso}}(r_{\text{o}})$ in (4) and the minimum node degree distribution $f_D(k; r_{\text{o}})$ in (5). $F(\boldsymbol{u}; r_{\text{o}})$ is a function of both the node location $\boldsymbol{u}$ and the transmission range r_{o}. For a unit square, if $r_{\text{o}} \geq \sqrt{2}$, then the disk $\mathcal{O}(\boldsymbol{u}; r_{\text{o}})$ will cover the whole square $\mathcal{R}$ and hence $F(\boldsymbol{u}; r_{\text{o}}) = 1$, irrespective of the node location. For intermediate values of the node range $0 \leq r_{\text{o}} \leq \sqrt{2}$, both $\boldsymbol{u}$ and r_{o} need to be taken into account in determining $F(\boldsymbol{u}; r_{\text{o}})$. This adds further complexity to the task of evaluating (4) and (5). A tractable exact solution to this problem is presented in the next section.

III. Proposed Framework

A. Boundary Effects

We use the approach suggested in [33] in order to quantify the overlap area $|\mathcal{O}(\boldsymbol{u}; r_{\text{o}}) \cap \mathcal{R}|$. The basic building blocks in this approach to characterize the boundary effects are (i) the circular segment areas formed outside each side (*border*

This article has been accepted for publication in a future issue of this journal, but has not been fully edited. Content may change prior to final publication. Citation information: DOI 10.1109/TVT.2013.2293580, IEEE Transactions on Vehicular Technology

effects) and (ii) the corner overlap areas between two circular segments formed at each vertex (*corner effects*). We modify the approach in [33] by placing the origin at the vertex V_1, rather than at the center of the square. This leads to a simpler formulation, as discussed below.

Let $B_1(\boldsymbol{u}; r_{\rm o})$ denote the area of the circular segment formed outside the side S_1, as illustrated in Fig. 1. Using the fact that the area of the circular segment is equal to the area of the circular sector minus the area of the triangular portion, we obtain

$$B_1(\boldsymbol{u}; r_{\rm o}) = \begin{cases} r_{\rm o}^2 \arccos\left(\frac{x}{r_{\rm o}}\right) - \\ \quad x\sqrt{r_{\rm o}^2 - x^2} & \Delta_s(\boldsymbol{u}, S_1) = x \geq r_{\rm o}, \\ 0 & \text{otherwise}, \end{cases} \tag{7}$$

where $\Delta_s(\boldsymbol{u}, S_\ell)$ denotes the Euclidean distance between $\boldsymbol{u}$ and side S_ℓ, $\ell = 1, 2, 3, 4$. Similarly, the areas of the circular segments formed outside the sides S_2, S_3 and S_4, respectively, can be expressed as

$$B_2(\boldsymbol{u}; r_{\rm o}) = r_{\rm o}^2 \arccos\left(\frac{y}{r_{\rm o}}\right) - y\sqrt{r_{\rm o}^2 - y^2}, \tag{8}$$

$$B_3(\boldsymbol{u}; r_{\rm o}) = r_{\rm o}^2 \arccos\left(\frac{1-x}{r_{\rm o}}\right) - (1-x)\sqrt{r_{\rm o}^2 - (1-x)^2}, \tag{9}$$

$$B_4(\boldsymbol{u}; r_{\rm o}) = r_{\rm o}^2 \arccos\left(\frac{1-y}{r_{\rm o}}\right) - (1-y)\sqrt{r_{\rm o}^2 - (1-y)^2}. \tag{10}$$

Let $C_1(\boldsymbol{u}; r_{\rm o})$ denote the area of the corner overlap region between two circular segments at vertex V_1, as illustrated in Fig. 1. Using the fact that the area of the overlap region is equal to the area of the circular sector minus the area of two triangular portions, we can easily show that

$$C_1(\boldsymbol{u}; r_{\rm o}) = \frac{1}{2} r_{\rm o}^2 \theta - \frac{1}{2}\left(\sqrt{r_{\rm o}^2 - y^2} - x\right) y - \frac{1}{2}\left(\sqrt{r_{\rm o}^2 - x^2} - y\right) x, \tag{11}$$

where the angle θ is given by

$$\theta = 2 \arcsin\left(\frac{\text{abs}\left(\sqrt{\theta_1}\right)}{2r_{\rm o}}\right), \tag{12}$$

where $\text{abs}(\cdot)$ denotes the absolute value or modulus and $\theta_1 = 2r_{\rm o}^2 - 2x\sqrt{r_{\rm o}^2 - y^2} - 2y\sqrt{r_{\rm o}^2 - x^2}$. Similarly, the areas of the corner overlap region formed at vertex V_2, V_3 and V_4, respectively, can be expressed as

$$C_2(\boldsymbol{u}; r_{\rm o}) = \frac{1}{2} r_{\rm o}^2 \alpha - \frac{1}{2}\left(\sqrt{r_{\rm o}^2 - y^2} - (1-x)\right) y - \frac{1}{2}\left(\sqrt{r_{\rm o}^2 - (1-x)^2} - y\right)(1-x), \tag{13}$$

$$C_3(\boldsymbol{u}; r_{\rm o}) = \frac{1}{2} r_{\rm o}^2 \beta - \frac{1}{2}\left(\sqrt{r_{\rm o}^2 - (1-y)^2} - (1-x)\right)(1-y) - \frac{1}{2}\left(\sqrt{r_{\rm o}^2 - (1-x)^2} - (1-y)\right)(1-x), \tag{14}$$

$$C_4(\boldsymbol{u}; r_{\rm o}) = \frac{1}{2} r_{\rm o}^2 \gamma - \frac{1}{2}\left(\sqrt{r_{\rm o}^2 - (1-y)^2} - x\right)(1-y) - \frac{1}{2}\left(\sqrt{r_{\rm o}^2 - x^2} - (1-y)\right) x, \tag{15}$$

where the angles α, β and γ are given by

$$\alpha = 2 \arcsin\left(\frac{\text{abs}\left(\sqrt{\alpha_1}\right)}{2r_{\rm o}}\right) \tag{16}$$

$$\beta = 2 \arcsin\left(\frac{\text{abs}\left(\sqrt{\beta_1}\right)}{2r_{\rm o}}\right) \tag{17}$$

$$\gamma = 2 \arcsin\left(\frac{\text{abs}\left(\sqrt{\gamma_1}\right)}{2r_{\rm o}}\right) \tag{18}$$

where $\alpha_1 = 2r_{\rm o}^2 - 2(1-x)\sqrt{r_{\rm o}^2 - y^2} - 2y\sqrt{r_{\rm o}^2 - (1-x)^2}$, $\beta_1 = 2r_{\rm o}^2 - 2(1-x)\sqrt{r_{\rm o}^2 - (1-y)^2} - 2(1-y)\sqrt{r_{\rm o}^2 - (1-x)^2}$ and $\gamma_1 = 2r_{\rm o}^2 - 2x\sqrt{r_{\rm o}^2 - (1-y)^2} - 2(1-y)\sqrt{r_{\rm o}^2 - x^2}$. We note that the expressions for $C_\ell(\boldsymbol{u}; r_{\rm o})$ are valid only when $\Delta_s(\boldsymbol{u}, V_\ell) \geq r_{\rm o}$, where $\Delta_s(\boldsymbol{u}, V_\ell)$ denotes the Euclidean distance between $\boldsymbol{u}$ and vertex V_ℓ, $\ell = 1, 2, 3, 4$.. For the case when $\Delta_s(\boldsymbol{u}, V_\ell) < r_{\rm o}$, $C_\ell(\boldsymbol{u}; r_{\rm o}) = 0$.

Using (7)−(10) and (11), (13)−(15), the CDF $F(\boldsymbol{u}; r_{\rm o})$ in (3) can be expressed in closed-form, e.g., if $r_{\rm o} = 0.1$ and $\boldsymbol{u} = (0, 0)$, then two circular segments are formed outside sides S_1 and S_2 and also there is overlap between them. Hence, in this case, $F(\boldsymbol{u}; r_{\rm o}) = \pi r_{\rm o}^2 - (B_1(\boldsymbol{u}; r_{\rm o}) + B_2(\boldsymbol{u}; r_{\rm o}) - C_1(\boldsymbol{u}; r_{\rm o}))$. This will be further illustrated in the next subsection.

B. Tractable Framework

As illustrated in the last subsection, for a given value of the transmission range $r_{\rm o}$ and the location of the arbitrary node $\boldsymbol{u}$, $F(\boldsymbol{u}; r_{\rm o})$ can be expressed in closed-form using (7)−(10) and (11), (13)−(15). In order to facilitate the averaging of (3) over the whole square region, we divide the square region into different non-overlapping subregions based on the different border and corner effects that occur in that region. Due to the symmetry of the square, some subregions have the same number of border and corner effects which can be exploited to further simplify the averaging. This will be elaborated in detail shortly.

Let $\mathcal{R}_1$, $\mathcal{R}_2$, ... $\mathcal{R}_M$ denote the type of non-overlapping subregions and n_i, $i \in \{1, 2 \ldots, M\}$ denote the number of subregion of type $\mathcal{R}_i$. If $F_i(\boldsymbol{u}; r_{\rm o})$ denotes the conditional probability of connectivity for a node located at $\boldsymbol{u} \in \mathcal{R}_i$, we can write the probability of node isolation in (4) as

$$P_{\rm iso}(r_{\rm o}) = \sum_{i=1}^{M} n_i \int_{\mathcal{R}_i} \left(1 - F_i(\boldsymbol{u}; r_{\rm o})\right)^{N-1} ds(\boldsymbol{u}), \tag{19}$$

and the minimum node degree distribution $f_D(k; r_{\rm o})$ in (5) as

$$f_D(k; r_{\rm o}) = \text{P}(D = k) = \left(1 - \sum_{d=0}^{k-1} \sum_{i=1}^{M} n_i \binom{N-1}{d} \times \int_{\mathcal{R}_i} \left(F(\boldsymbol{u}; r_{\rm o})\right)^d \left(1 - F(\boldsymbol{u}; r_{\rm o})\right)^{n-d-1} ds(\boldsymbol{u})\right)^N. \tag{20}$$

We note that the average node degree denoted by $\overline{D}$ can

This article has been accepted for publication in a future issue of this journal, but has not been fully edited. Content may change prior to final publication. Citation information: DOI 10.1109/TVT.2013.2293580, IEEE Transactions on Vehicular Technology

also be determined using our framework as [14]

$$\overline{D} = (N-1)\int_{\mathcal{R}} F(\boldsymbol{u}; r_{\rm o}) ds(\boldsymbol{u}) = (N-1)\sum_{i=1}^{M} n_i \int_{\mathcal{R}_i} F(\boldsymbol{u}; r_{\rm o}) ds(\boldsymbol{u}). \quad (21)$$

In fact $\int_{\mathcal{R}} F(\boldsymbol{u}; r_{\rm o}) ds(\boldsymbol{u})$ in (21) denotes the cumulative distribution function of the distance between two randomly placed nodes and the closed form analytical results exist in the literature for square, hexagon [6] and convex regular polygons [34].

Remark 1: The general formulation for $P_{\rm iso}(r_{\rm o})$ in (4) is also indirectly suggested in [25]. However, no guidelines are presented in order to evaluate (4). Hence, the authors in [25] use a deterministic grid deployment of nodes to approximate the boundary effects when nodes are uniformly and independently distributed in a square region. By contrast, we provide a tractable framework for complete and exact characterization of the boundary effects in (19).

Remark 2: While $F_i(\boldsymbol{u}; r_{\rm o})$ in (3) can be expressed analytically in closed-form, the integration in (19) and (20) does not have a closed-form due to the $N-1$ factor in the exponent. However, it can be easily evaluated numerically using the explicit closed-form expressions for $F_i(\boldsymbol{u}; r_{\rm o})$ for different transmission ranges and different subregions. It must be noted that numerical evaluation of two-fold integrals is widely practiced in the literature [35].

Remark 3: We have considered a unit square region for the sake of simplicity in the proposed formulation. For the general case of a square of side length L, (19)-(21) can be used with appropriate scaling of the transmission range as $r_{\rm o} \to r_{\rm o}/L$.

Since the subregions are classified on the basis of the boundary effects, the subregions change with the transmission range $r_{\rm o}$. We divide the range $r_{\rm o}$ over the desired interval $0 \le r_{\rm o} \le \sqrt{2}$, as explained in Section II-C, such that the boundary effects are the same for the different subregions over each subinterval of the transmission range. This is explained in detail in the next section.

IV. Effect of Boundaries for the Different Transmission Range Cases

A. Transmission Range - $0 \le r_o \le 1/2$

Consider the first case of the transmission range, i.e., $0 \le r_{\rm o} \le \frac{1}{2}$, as shown in Fig. 2. This case may be of greatest interest in many practical situations where typically the sensor transmission range is a small fraction of the side length of the square. In this case, we can divide the square into four ($M = 4$) types of subregions $\mathcal{R}_1$, $\mathcal{R}_2$, $\mathcal{R}_3$ and $\mathcal{R}_4$. As shown in Fig. 2, although there is one subregion of type $\mathcal{R}_1$, there are four subregions of types $\mathcal{R}_2$, $\mathcal{R}_3$ and $\mathcal{R}_4$, respectively, which are shaded in the same color for ease of identification, e.g., for an arbitrary node located in any subregion of type $\mathcal{R}_2$, the disk $\mathcal{O}(\boldsymbol{u}; r_{\rm o})$ is limited by one side only. Hence, we determine $F_i(\boldsymbol{u}; r_{\rm o})$ only for the following subregions

- $\mathcal{R}_1 = \{x \in (r_{\rm o}, 1-r_{\rm o}),\, y \in (r_{\rm o}, 1-r_{\rm o})\}$
- $\mathcal{R}_2 = \{x \in (0, r_{\rm o}),\, y \in (r_{\rm o}, 1-r_{\rm o})\}$

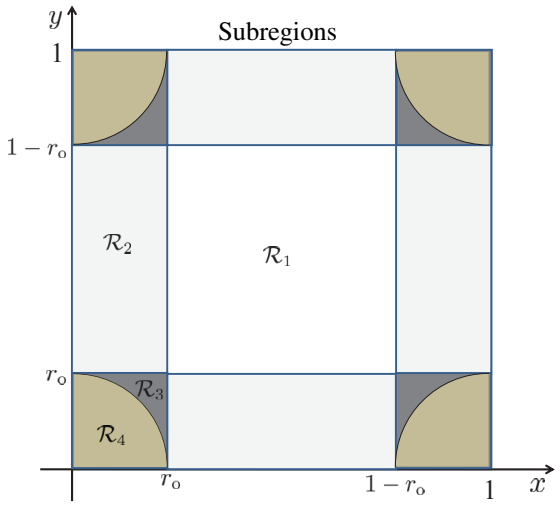

TABLE I

$\mathcal{R}_i$	n_i	$F_i(\boldsymbol{u}; r_{\rm o})$
$\mathcal{R}_1$	1	$\pi r_{\rm o}^2$
$\mathcal{R}_2$	4	$\pi r_{\rm o}^2 - (B_1)$
$\mathcal{R}_3$	4	$\pi r_{\rm o}^2 - (B_1 + B_2)$
$\mathcal{R}_4$	4	$\pi r_{\rm o}^2 - (B_1 + B_2 - C_1)$

Fig. 2: Subregions for transmission range $0 \le r_{\rm o} \le \frac{1}{2}$ are shown in the figure (top) and conditional probabilities $F_i(\boldsymbol{u}; r_{\rm o})$ and number of subregions n_i for each subregion are shown in the Table I (bottom).

- $\mathcal{R}_3 = \{x \in (0, r_{\rm o}),\, y \in (\sqrt{r_{\rm o}^2 - x^2}, r_{\rm o})\}$
- $\mathcal{R}_4 = \{x \in (0, r_{\rm o}),\, y \in (0, \sqrt{r_{\rm o}^2 - x^2})\}$

It is easy to see that for an arbitrary node located anywhere in subregion $\mathcal{R}_1$, the disk $\mathcal{O}(\boldsymbol{u}; r_{\rm o})$ is completely inside the square $\mathcal{R}$, i.e., there are no border or corner effects. Hence, $F_1(\boldsymbol{u}; r_{\rm o}) = \pi r_{\rm o}^2$. For an arbitrary node located anywhere in subregion $\mathcal{R}_2$, the disk $\mathcal{O}(\boldsymbol{u}; r_{\rm o})$ is limited by side S_1, i.e., there is a circular segment formed outside the side S_1. Hence, $F_2(\boldsymbol{u}; r_{\rm o}) = \pi r_{\rm o}^2 - (B_1(\boldsymbol{u}; r_{\rm o}))$. For an arbitrary node located anywhere in subregion $\mathcal{R}_3$, the disk $\mathcal{O}(\boldsymbol{u}; r_{\rm o})$ is limited by sides S_1 and S_2, i.e., there is are two circular segments formed outside the sides S_1 and S_2 and there is no corner overlap between them. Hence, $F_3(\boldsymbol{u}; r_{\rm o}) = \pi r_{\rm o}^2 - (B_1(\boldsymbol{u}; r_{\rm o}) + B_2(\boldsymbol{u}; r_{\rm o}))$. For an arbitrary node located anywhere in subregion $\mathcal{R}_4$, the disk $\mathcal{O}(\boldsymbol{u}; r_{\rm o})$ is limited by sides S_1 and S_2 and vertex V_1, i.e., there is are two circular segments formed outside the sides S_1 and S_2 and there is corner overlap between them. Hence, $F_4(\boldsymbol{u}; r_{\rm o}) = \pi r_{\rm o}^2 - (B_1(\boldsymbol{u}; r_{\rm o}) + B_2(\boldsymbol{u}; r_{\rm o}) - C_1(\boldsymbol{u}; r_{\rm o}))$. The number of subregions n_i of each type and the corresponding closed form $F_i(\boldsymbol{u}; r_{\rm o})$ are tabulated in Table I. For the sake of brevity, $B_\ell(u; r_0)$ and $C_\ell(u; r_0)$ are denoted as B_ℓ and C_ℓ, respectively in this and subsequent tables.

As $r_{\rm o}$ increases from 0 to $1/2$, we can see that the subregions of type $\mathcal{R}_1$ and $\mathcal{R}_2$ become smaller and the subregions of type $\mathcal{R}_3$ and $\mathcal{R}_4$ become larger. For the value of range $r_{\rm o} = \frac{1}{2}$, the subregions of type $\mathcal{R}_1$ and $\mathcal{R}_2$ approach zero.

This article has been accepted for publication in a future issue of this journal, but has not been fully edited. Content may change prior to final publication. Citation information: DOI 10.1109/TVT.2013.2293580, IEEE Transactions on Vehicular Technology

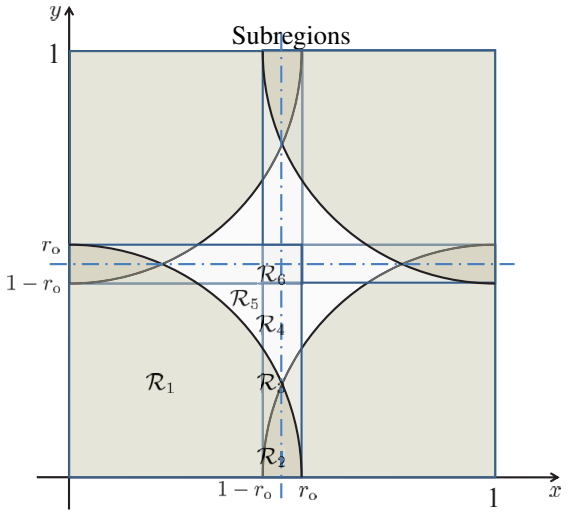

TABLE II

$\mathcal{R}_i$	n_i	$F_i(\boldsymbol{u}; r_o)$
$\mathcal{R}_1$	4	$\pi r_o^2 - (B_1 + B_2 - C_1)$
$\mathcal{R}_2$	8	$\pi r_o^2 - (B_1 + B_2 + B_3 - C_1 - C_2)$
$\mathcal{R}_3$	8	$\pi r_o^2 - (B_1 + B_2 + B_3 - C_1)$
$\mathcal{R}_4$	8	$\pi r_o^2 - (B_1 + B_2 + B_3)$
$\mathcal{R}_5$	4	$\pi r_o^2 - (B_1 + B_2)$
$\mathcal{R}_6$	4	$\pi r_o^2 - (B_1 + B_2 + B_3 + B_4)$

Fig. 3: Subregions for transmission range $1/2 \leq r_o \leq (2 - \sqrt{2})$ are shown in the figure (top) and conditional probabilities $F_i(\boldsymbol{u}; r_o)$ and number of subregions n_i for each subregion are shown in the Table II (bottom).

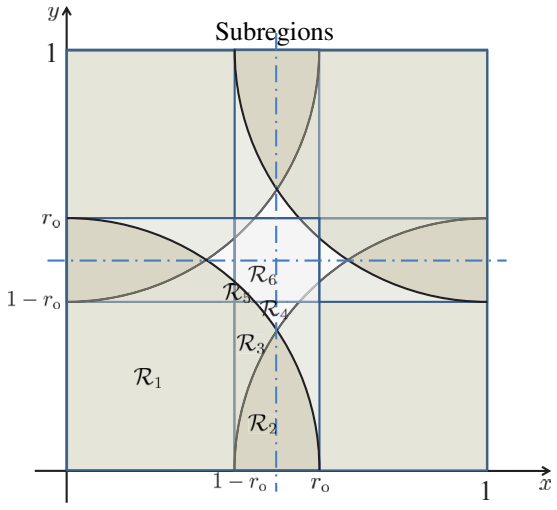

TABLE III

$\mathcal{R}_i$	n_i	$F_i(\boldsymbol{u}; r_o)$
$\mathcal{R}_1$	4	$\pi r_o^2 - (B_1 + B_2 - C_1)$
$\mathcal{R}_2$	8	$\pi r_o^2 - (B_1 + B_2 + B_3 - C_1 - C_2)$
$\mathcal{R}_3$	8	$\pi r_o^2 - (B_1 + B_2 + B_3 - C_1)$
$\mathcal{R}_4$	8	$\pi r_o^2 - (B_1 + B_2 + B_3)$
$\mathcal{R}_5$	4	$\pi r_o^2 - (B_1 + B_2 + B_3 + B_4 - C_1)$
$\mathcal{R}_6$	4	$\pi r_o^2 - (B_1 + B_2 + B_3 + B_4)$

Fig. 4: Subregions for transmission range $(2 - \sqrt{2}) \leq r_o \leq 5/8$ are shown in the figure (top) and conditional probabilities $F_i(\boldsymbol{u}; r_o)$ and number of subregions n_i for each subregion are shown in the Table III (bottom).

Remark 4: The division of the square $\mathcal{R}$ into subregions for transmission range $0 \leq r_o \leq 1/2$ has been previously shown in [25, Fig. 7], [26, Fig. 2] and [29, Fig. 2] to illustrate the intuitive argument that the nodes situated in boundary subregions experience border effects. However, subregions $\mathcal{R}_3$ and $\mathcal{R}_4$ are indicated as one subregion in [25], [26]. Using our framework, we show that these are two distinct subregions with unique border and corner effects. In addition, we formulate all the subregions for all possible values of the range. This is different to [29], [36] where only the transmission range $0 \leq r_o \leq 1/2$ was considered for finding the average node degree.

B. Transmission Range - $1/2 \leq r_o \leq (2 - \sqrt{2})$

For the case of the transmission range in the interval $1/2 \leq r_o \leq 2 - \sqrt{2}$, we have $M = 6$ types of subregions, which are shown in Fig. 3 and can be expressed as

- $\mathcal{R}_1 = \{x \in (0, \sqrt{2r_o - 1}), y \in (0, 1 - r_o)\} \cup \{x \in (\sqrt{2r_o - 1}, 1 - r_o), y \in (0, \sqrt{r_o^2 - x^2})\}$
- $\mathcal{R}_2 = \{x \in (1 - r_o, 0.5), y \in (0, \sqrt{r_o^2 - (x-1)^2})\}$
- $\mathcal{R}_3 = \{x \in (1 - r_o, 0.5), y \in (\sqrt{r_o^2 - (x-1)^2}, \sqrt{r_o^2 - x^2})\}$
- $\mathcal{R}_4 = \{x \in (1 - r_o, 0.5), y \in (\sqrt{r_o^2 - x^2}, 1 - r_o)\}$
- $\mathcal{R}_5 = \{x \in (\sqrt{2r_o - 1}, 1 - r_o), y \in (\sqrt{r_o^2 - x^2}, 1 - r_o)\}$
- $\mathcal{R}_6 = \{x \in (1 - r_o, 0.5), y \in (1 - r_o, 0.5)\}$

The upper limit for this interval of transmission range, i.e., $(2 - \sqrt{2})$ is computed as the range r_o for which the lines $x = 1 - r_o$, $y = 1 - r_o$ and circle $x^2 + y^2 = r_o^2$ intersect. As r_o approaches $(2 - \sqrt{2})$, the subregion $\mathcal{R}_5$ squeezes to zero. The number of subregions n_i of each type and the corresponding closed-form $F_i(\boldsymbol{u}; r_o)$ are tabulated in Table II.

C. Transmission Range - $(2 - \sqrt{2}) \leq r_o \leq 5/8$

For the case of the transmission range in the interval $(2 - \sqrt{2}) \leq r_o \leq 5/8$, we again have $M = 6$ types of subregions, which are shown in Fig. 4 and can be expressed as

- $\mathcal{R}_1 = \{x \in (0, 1 - r_o), y \in (0, 1 - r_o)\}$
- $\mathcal{R}_2 = \{x \in (1 - r_o, 0.5), y \in (0, \sqrt{r_o^2 - (x-1)^2})\}$
- $\mathcal{R}_3 = \{x \in (1 - r_o, \sqrt{2r_o - 1}), y \in (\sqrt{r_o^2 - (x-1)^2}, 1 - r_o)\} \cup \{x \in (\sqrt{2r_o - 1}, 0.5), y \in (\sqrt{r_o^2 - (x-1)^2}, \sqrt{r_o^2 - x^2})\}$
- $\mathcal{R}_4 = \{x \in (\sqrt{2r_o - 1}, 0.5), y \in (\sqrt{r_o^2 - x^2}, 1 - r_o)\}$
- $\mathcal{R}_5 = \{x \in (1 - r_o, \sqrt{2r_o - 1}), y \in (1 - r_o, \sqrt{r_o^2 - x^2})\}$
- $\mathcal{R}_6 = \{x \in (1 - r_o, \sqrt{2r_o - 1}), y \in (\sqrt{r_o^2 - x^2}, 0.5)\} \cup \{x \in (\sqrt{2r_o - 1}, 0.5), y \in (1 - r_o, 0.5)\}$

The upper limit for this interval of the transmission range, i.e., $5/8$ is determined as the range r_o where the subregion $\mathcal{R}_4$ squeezes to zero and is computed as an intersection of the line $y = 1 - r_o$ and two circles $x^2 + y^2 = r_o^2$ and $(x-1)^2 +$

This article has been accepted for publication in a future issue of this journal, but has not been fully edited. Content may change prior to final publication. Citation information: DOI 10.1109/TVT.2013.2293580, IEEE Transactions on Vehicular Technology

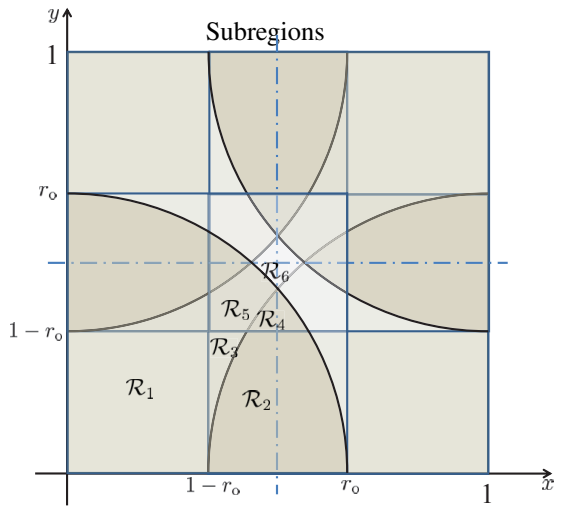

TABLE IV

$\mathcal{R}_i$	n_i	$F_i(\boldsymbol{u}; r_o)$
$\mathcal{R}_1$	4	$\pi r_o^2 - (B_1 + B_2 - C_1)$
$\mathcal{R}_2$	8	$\pi r_o^2 - (B_1 + B_2 + B_3 - C_1 - C_2)$
$\mathcal{R}_3$	8	$\pi r_o^2 - (B_1 + B_2 + B_3 - C_1)$
$\mathcal{R}_4$	8	$\pi r_o^2 - (B_1 + B_2 + B_3 + B_4 - C_1 - C_2)$
$\mathcal{R}_5$	4	$\pi r_o^2 - (B_1 + B_2 + B_3 + B_4 - C_1)$
$\mathcal{R}_6$	4	$\pi r_o^2 - (B_1 + B_2 + B_3 + B_4)$

Fig. 5: Subregions for transmission range $5/8 \leq r_o \leq 1/\sqrt{2}$ are shown in the figure (top) and conditional probabilities $F_i(\boldsymbol{u}; r_o)$ and number of subregions n_i for each subregion are shown in the Table IV (bottom).

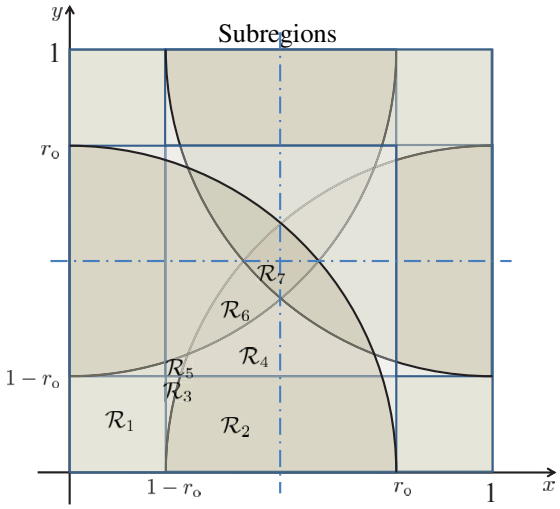

TABLE V

$\mathcal{R}_i$	n_i	$F_i(\boldsymbol{u}; r_o)$
$\mathcal{R}_1$	4	$\pi r_o^2 - (B_1 + B_2 - C_1)$
$\mathcal{R}_2$	8	$\pi r_o^2 - (B_1 + B_2 + B_3 - C_1 - C_2)$
$\mathcal{R}_3$	8	$\pi r_o^2 - (B_1 + B_2 + B_3 - C_1)$
$\mathcal{R}_4$	8	$\pi r_o^2 - (B_1 + B_2 + B_3 + B_4 - C_1 - C_2)$
$\mathcal{R}_5$	4	$\pi r_o^2 - (B_1 + B_2 + B_3 + B_4 - C_1)$
$\mathcal{R}_6$	4	$\pi r_o^2 - (B_1 + B_2 + B_3 + B_4 - C_1 - C_2 - C_4)$
$\mathcal{R}_7$	4	$\pi r_o^2 - (B_1 + B_2 + B_3 + B_4 - C_1 - C_2 - C_3 - C_4) = 1$

Fig. 6: Subregions for transmission range $1/\sqrt{2} \leq r_o \leq 1$ are shown in the figure (top) and conditional probabilities $F_i(\boldsymbol{u}; r_o)$ and number of subregions n_i for each subregion are shown in the Table V (bottom).

$y^2 = r_o^2$. The number of subregions n_i of each type and the corresponding closed-form $F_i(\boldsymbol{u}; r_o)$ are tabulated in Table III.

D. Transmission Range - $5/8 \leq r_o \leq 1/\sqrt{2}$

For the case of the transmission range in the interval $5/8 \leq r_o \leq 1/\sqrt{2}$, we have $M = 6$ types of subregions, which are shown in Fig. 5 and can be expressed as

- $\mathcal{R}_1 = \{x \in (0, 1-r_o),\, y \in (0, 1-r_o)\}$
- $\mathcal{R}_2 = \{x \in (1-\sqrt{r_o^2 - y^2}, 0.5),\, y \in (0, 1-r_o)\}$
- $\mathcal{R}_3 = \{x \in (1-r_o, 1-\sqrt{r_o^2 - y^2}),\, y \in (0, 1-r_o)\}$
- $\mathcal{R}_4 = \{x \in (1-\sqrt{2r_o - 1}, 0.5),\, y \in (1-r_o, \sqrt{r_o^2 - (x-1)^2})\}$
- $\mathcal{R}_5 = \{x \in (1-r_o, \sqrt{r_o^2 - 0.25}),\, y \in (1-r_o, 1-\sqrt{r_o^2 - x^2})\} \cup \{x \in (\sqrt{r_o^2 - 0.25}, 1-\sqrt{2r_o - 1}),\, y \in (1-r_o, \sqrt{r_o^2 - x^2})\} \cup \{x \in (1-\sqrt{2r_o - 1}, 0.5),\, y \in (\sqrt{r_o^2 - (x-1)^2}, \sqrt{r_o^2 - x^2})\}$
- $\mathcal{R}_6 = \{x \in (\sqrt{r_o^2 - 0.25}, 0.5),\, y \in (\sqrt{r_o^2 - x^2}, 0.5)\}$

The upper limit for this interval of the transmission range, i.e., $1/\sqrt{2}$ is determined as the range r_o where the four circles $x^2 + y^2 = r_o^2$, $(x-1)^2 + y^2 = r_o^2$, $(x-1)^2 + (y-1)^2 = r_o^2$ and $(x)2 + (y-1)^2 = r_o^2$ intersect. The number of subregions n_i of each type and the corresponding closed-form $F_i(\boldsymbol{u}; r_o)$ are tabulated in Table IV.

E. Transmission Range - $1/\sqrt{2} \leq r_o \leq 1$

For the case of the transmission range in the interval $1/\sqrt{2} \leq r_o \leq 1$, we have $M = 7$ types of subregions, which are shown in Fig. 6 and can be expressed as

- $\mathcal{R}_1 = \{x \in (0, 1-r_o),\, y \in (0, 1-r_o)\}$
- $\mathcal{R}_2 = \{x \in (1-r_o, 1-\sqrt{2r_o - 1}),\, y \in (0, \sqrt{r_o^2 - (x-1)^2})\} \cup \{x \in (1-\sqrt{2r_o - 1}, 0.5),\, y \in (0, 1-r_o)\}$
- $\mathcal{R}_3 = \{x \in (1-r_o, 1-\sqrt{2r_o - 1}),\, y \in (\sqrt{r_o^2 - (x-1)^2}, 1-r_o)\}$
- $\mathcal{R}_4 = \{x \in (1-\sqrt{2r_o - 1}, (1-\sqrt{2r_o^2 - 1})/2),\, y \in (1-r_o, \sqrt{r_o^2 - (x-1)^2})\} \cup \{x \in ((1-\sqrt{2r_o^2 - 1})/2, 0.5),\, y \in (1-r_o, 1-\sqrt{r_o^2 - x^2})\}$
- $\mathcal{R}_5 = \{x \in (1-r_o, 1-\sqrt{2r_o - 1}),\, y \in (1-r_o, 1-\sqrt{r_o^2 - x^2})\} \cup \{x \in (1-\sqrt{2r_o - 1}, (1-\sqrt{2r_o^2 - 1})/2),\, y \in (\sqrt{r_o^2 - (x-1)^2}, 1-\sqrt{r_o^2 - x^2})\}$
- $\mathcal{R}_6 = \{x \in ((1-\sqrt{2r_o^2 - 1})/2, 1-\sqrt{r_o^2 - 0.25}),\, y \in (1-\sqrt{r_o^2 - x^2}, \sqrt{r_o^2 - (x-1)^2})\} \cup \{x \in (1-\sqrt{r_o^2 - 0.25}, 0.5),\, y \in (1-\sqrt{r_o^2 - x^2}, 1-\sqrt{r_o^2 - (x-1)^2})\}$
- $\mathcal{R}_7 = \{x \in (1-\sqrt{r_o^2 - 0.25}, 0.5),\, y \in (1-\sqrt{r_o^2 - (x-1)^2}, 0.5)\}$

The upper limit for this interval of the transmission range, i.e., 1 corresponds to the length of the side of the square region.

This article has been accepted for publication in a future issue of this journal, but has not been fully edited. Content may change prior to final publication. Citation information: DOI 10.1109/TVT.2013.2293580, IEEE Transactions on Vehicular Technology

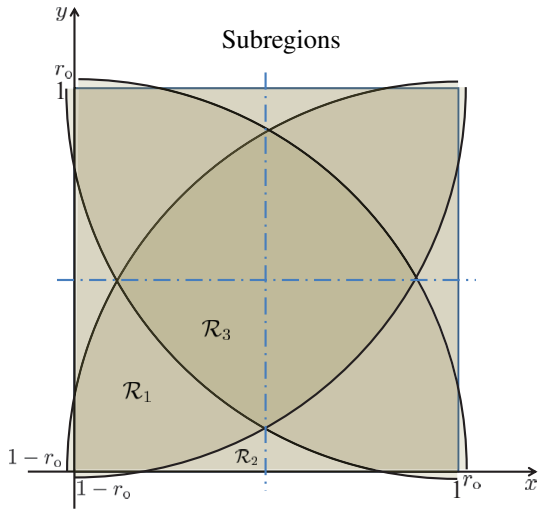

TABLE VI

$\mathcal{R}_i$	n_i	$F_i(\boldsymbol{u}; r_o)$
$\mathcal{R}_1$	4	$\pi r_o^2 - (B_1 + B_2 + B_3 + B_4 - C_1 - C_2 - C_4)$
$\mathcal{R}_2$	8	$\pi r_o^2 - (B_1 + B_2 + B_3 + B_4 - C_1 - C_2)$
$\mathcal{R}_3$	4	$\pi r_o^2 - (B_1 + B_2 + B_3 + B_4 - C_1 - C_2 - C_3 - C_4) = 1$

Fig. 7: Subregions for transmission range $1 \leq r_o \leq \sqrt{5}/2$ are shown in the figure (top) and conditional probabilities $F_i(\boldsymbol{u}; r_o)$ and number of subregions n_i for each subregion are shown in the Table VI (bottom).

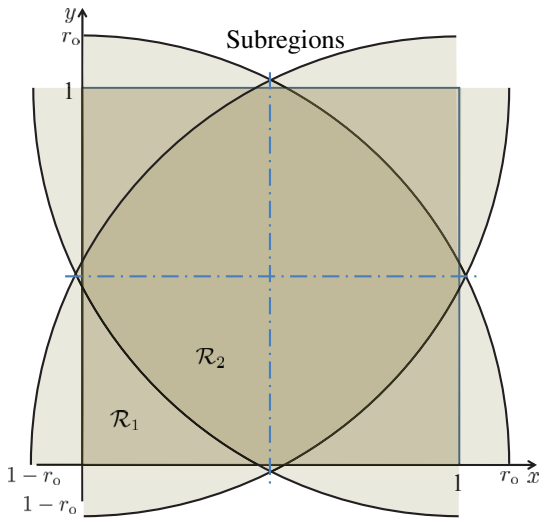

TABLE VII

$\mathcal{R}_i$	n_i	$F_i(\boldsymbol{u}; r_o)$
$\mathcal{R}_1$	4	$\pi r_o^2 - (B_1 + B_2 + B_3 + B_4 - C_1 - C_2 - C_4)$
$\mathcal{R}_2$	4	$\pi r_o^2 - (B_1 + B_2 + B_3 + B_4 - C_1 - C_2 - C_3 - C_4) = 1$

Fig. 8: Subregions for transmission range $\sqrt{5}/2 \leq r_o \leq \sqrt{2}$ are shown in the figure (top) and conditional probabilities $F_i(\boldsymbol{u}; r_o)$ and number of subregions n_i for each subregion are shown in the Table VII (bottom).

For $r_o \geq 1$, there is always the effect of the sides of the square on the coverage area of a node irrespective of the location of the node. The number of subregions n_i of each type and the corresponding closed-form $F_i(\boldsymbol{u}; r_o)$ are tabulated in Table V.

F. Transmission Range - $1 \leq r_o \leq \sqrt{5}/2$

For the case of the transmission range in the interval $1 \leq r_o \leq \sqrt{5}/2$, we have $M = 3$ types of subregions, which are shown in Fig. 7 and can be expressed as

- $\mathcal{R}_1 = \{x \in (0, 1 - \sqrt{r_o^2 - 0.25}), y \in (0, \sqrt{r_o^2 - (x-1)^2})\} \cup \{x \in (1 - \sqrt{r_o^2 - 0.25}, \sqrt{r_o^2 - 1}), y \in (0, 1 - \sqrt{r_o^2 - (x-1)^2})\} \cup \{x \in (\sqrt{r_o^2 - 1}, 0.5), y \in (1 - \sqrt{r_o^2 - x^2}, 1 - \sqrt{r_o^2 - (x-1)^2})\}$
- $\mathcal{R}_2 = \{x \in (\sqrt{r_o^2 - 1}, 0.5), y \in (0, 1 - \sqrt{r_o^2 - x^2})\}$
- $\mathcal{R}_3 = \{x \in (1 - \sqrt{r_o^2 - 0.25}, 0.5), y \in (1 - \sqrt{r_o^2 - (x-1)^2}, 0.5)\}$

The upper limit for this interval of the transmission range, i.e., $\sqrt{5}/2$ is determined as r_o for which the circles $(x-1)^2 + (y-1)^2 = r_o^2$, $x^2 + (y-1)^2 = r_o^2$ intersect and the subregion $\mathcal{R}_2$ vanishes. The number of subregions n_i of each type and the corresponding closed-form $F_i(\boldsymbol{u}; r_o)$ are tabulated in Table VI.

G. Transmission Range - $\sqrt{5}/2 \leq r_o \leq \sqrt{2}$

Finally, we have $M = 2$ types of subregions for the case of the transmission range in the interval $\sqrt{5}/2 \leq r_o \leq \sqrt{2}$. The regions are shown in Fig. 8 and can be expressed as

- $\mathcal{R}_1 = \{x \in (0, 1 - \sqrt{r_o^2 - 1}), y \in (0, 1 - \sqrt{r_o^2 - (x-1)^2})\}$
- $\mathcal{R}_2 = \{x \in (0, 1 - \sqrt{r_o^2 - 1}), y \in (1 - \sqrt{r_o^2 - (x-1)^2}, 0.5)\} \cup \{x \in (1 - \sqrt{r_o^2 - 1}, 0.5), y \in (0, 0.5)\}$

The number of subregions n_i of each type and the corresponding closed form $F_i(\boldsymbol{u}; r_o)$ are tabulated in Table VII. As highlighted earlier, we note that the $F(u : r_o) = 1$ for transmission range r_o greater than equal to $\sqrt{2}$ (diagonal length of the square).

V. Results

In this section, we present the numerical results and compare with the simulation results to validate the proposed framework. We also compare with the results from the prior work to demonstrate the advantage of our proposed framework, especially for smaller number of sensor nodes N. We have implemented (19) and (20) in Mathematica. We consider the nodes to be independently and uniformly distributed in a square region of side length $L = 1$. The simulation results are obtained by averaging over $S = 50,000$ Monte Carlo simulation runs.

A. Probability of Node Isolation

Fig. 9 plots the probability of node isolation, $P_{\text{iso}}(r_o)$, in (19), versus thetransmission range r_o for $N = 10, 20, 50$

This article has been accepted for publication in a future issue of this journal, but has not been fully edited. Content may change prior to final publication. Citation information: DOI 10.1109/TVT.2013.2293580, IEEE Transactions on Vehicular Technology

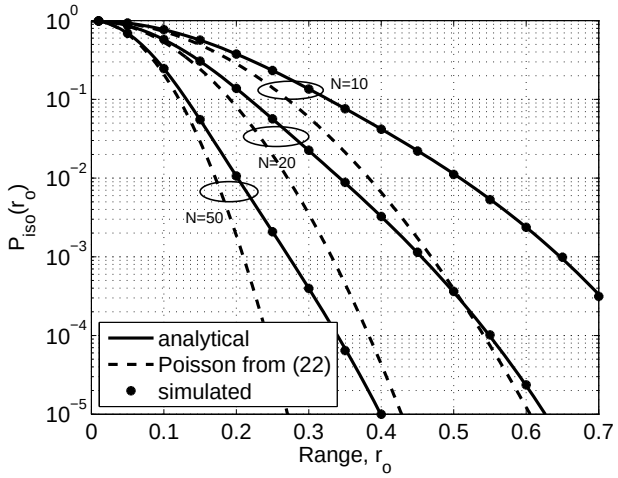

Fig. 9: Probability of node isolation, $P_{\text{iso}}(r_{\text{o}})$, versus the transmission range r_{o} for $N = 10, 20, 50$ nodes independently and uniformly distributed in a unit square.

nodes. The probability of node isolation in infinite homogenous Poisson point process networks [12]

$$P_{\text{iso}}(r_{\text{o}}) = e^{-\rho\pi r_{\text{o}}^2}, \tag{22}$$

assuming constant node density $\rho = 10, 20, 50$ nodes/m^2 is also plotted as a reference. We can see from Fig. 9 that the simulation results for finite networks match perfectly with the numerical results. This is to be expected since we account for boundary effects accurately and evaluate (19) exactly. Fig. 9 shows that the probability of node isolation is greater in finite networks, compared with Poisson networks. This is due to the inclusion of the border and corner effects, as explained in Section III.

B. Minimum Node Degree Distribution and k-Connectivity

Here, through simulations, we validate our framework to determine the minimum node degree distribution. Using (20), we determine the minimum node degree distribution $f_D(k; r_{\text{o}})$ for $k = 1, 2, 3$ and for number of nodes $N = 10, 20, 50$. The simulation results for $f_D(k; r_{\text{o}})$ are obtained by uniformly distributing the N nodes in a square region, each with transmission range r_{o}, over a square region and determining if the minimum of number of neighbors for all nodes in the network are equal to k. Note that the simulation results for $f_D(k; r_{\text{o}})$ are obtained by averaging over all $S = 50,000$ random topologies for each r_{o} and k . The simulation results for $f_D(k; r_{\text{o}})$ are also plotted in Fig. 10 and match perfectly with the analytical results using (20).

As highlighted earlier in Section II-B, the probability of k-connectivity $P_{\text{k-con}}(r_{\text{o}})$ is bounded by the minimum node degree distribution $f_D(k; r_{\text{o}})$. This is because we obtain a k-connected network at the same time when we obtain a network with minimum node degree k, both with and without boundary effects [12], [14], [15]. Here we validate through simulation results that the minimum node degree distribution $f_D(k; r_{\text{o}})$ serves as an upper bound for $P_{\text{k-con}}(r_{\text{o}})$ and the bound gets tighter as $P_{\text{k-con}}(r_{\text{o}})$ approaches one.

We repeat the simulation environment of Section V-B and now for each of the $50,000$ random topologies, we measure the k-connectivity of the network for $k = 1, 2, 3$. The simulation results for $P_{\text{k-con}}(r_{\text{o}})$ are plotted in Fig. 10 along with the analytical results for minimum node degree distribution $f_D(k; r_{\text{o}})$ obtained using (20) and our proposed framework. It is evident in the plots that the relation between $f_D(k; r_{\text{o}})$ and $P_{\text{k-con}}(r_{\text{o}})$ given in (6) holds, that is, $f_D(k; r_{\text{o}}) \to P_{\text{k-con}}(r_{\text{o}})$ as $P_{\text{k-con}}(r_{\text{o}}) \to 1$.

We note that the simulation tests for k-connectivity are computationally intensive and the computational complexity to check k-connectivity scales with N^{k-1} for $k \geq 2$. For example, the complexity to check 1-connectivity and 2-connectivity is of the order $O(N + S)$ and the complexity to determine 3-connectivity is $O(N(N+S))$, where S denotes the number of simulations. However, (20) can be evaluated numerically very easily. This illustrates an advantage of the proposed framework over simulations.

C. 1-Connectivity

Since $P_{\text{1-con}}(r_{\text{o}})$ is one of the essential characteristics of wireless multi-hop networks, we analyze the tightness of the bound provided by $f_D(1; r_{\text{o}})$ for $P_{\text{1-con}}(r_{\text{o}})$ in more detail and compare with the existing bounds in the literature.

Fig. 11 plots the $f_D(1; r_{\text{o}})$ as an upper bound for the probability of connectivity (obtained via simulations), versus transmission range r_{o} for $N = 10, 20, 50$ nodes. For comparison, we plot the high density approximation for $P_{\text{1-con}}(r_{\text{o}})$ which is derived in [27] using a cluster expansion approach as

$$\tilde{P}_{\text{1-con}}(r_{\text{o}}) \approx 1 - L^2\rho e^{-\frac{\pi}{\beta}\rho} - 4L\sqrt{\frac{\beta}{\pi}}e^{-\frac{\pi}{2\beta}\rho} - \frac{16\beta}{\rho\pi}e^{-\frac{\pi}{4\beta}\rho}, \tag{23}$$

where L denotes the side length, ρ denotes the node density and $\beta = (r_{\text{o}}/L)^{-2}$.

The high density approximation in (23) is comparatively a better estimate for $P_{\text{1-con}}(r_{\text{o}})$ for $N = 50$ nodes but is not useful for $N = 10$ nodes. We analyze the tightness of the bounds in more detail over the value of probabilities in the interval $0.9 \leq P_{\text{1-con}}(r_{\text{o}}) \leq 1$. The differences between the bounds, $\Delta = |P_{\text{1-con}}(r_{\text{o}}) - f_D(1; r_{\text{o}})|$ and $\tilde{\Delta} = |P_{\text{1-con}}(r_{\text{o}}) - \tilde{P}_{\text{1-con}}(r_{\text{o}})|$ is plotted in Fig. 12 for $0.9 \leq P_{\text{1-con}}(r_{\text{o}}) \leq 1$. For small number of nodes ($N = 10, 20$), it can be noted that the proposed minimum node degree distribution $f_D(1; r_{\text{o}})$ is comparatively a tight bound for $P_{\text{1-con}}(r_{\text{o}})$ than the high density approximation $\tilde{P}_{\text{1-con}}(r_{\text{o}})$.

On the basis of simulation results presented here and in the previous section, we can say that the upper bound for the connectivity provided by the minimum node degree distribution in (6) provides a good approximation for the simulation results when $P_{\text{1-con}}(r_{\text{o}}) \approx 1$. This is consistent with the observation in [14] for circular areas with or without boundary effects. Thus, the proposed framework can be used to accurately predict the network connectivity properties even when the number of nodes is small.

This article has been accepted for publication in a future issue of this journal, but has not been fully edited. Content may change prior to final publication. Citation information: DOI 10.1109/TVT.2013.2293580, IEEE Transactions on Vehicular Technology

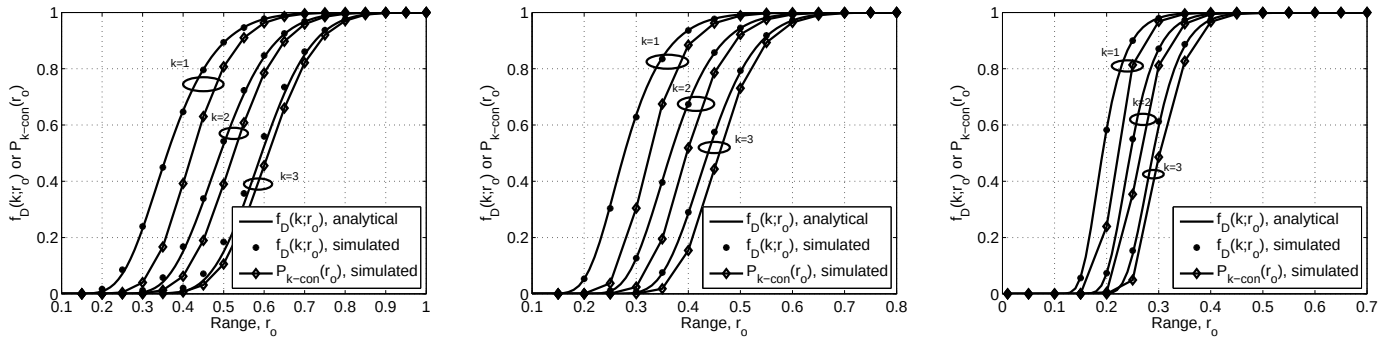

(a) $N = 10$ (b) $N = 20$ (c) $N = 50$

Fig. 10: Minimum node degree distribution, $f_D(k; r_{\rm o})$ and probability of k-connectivity, $P_{\text{1-con}}(r_{\rm o})$, versus transmission range $r_{\rm o}$ for (a) $N = 10$, (b) $N = 20$ and (c) $N = 50$ nodes independently and uniformly distributed in a unit square.

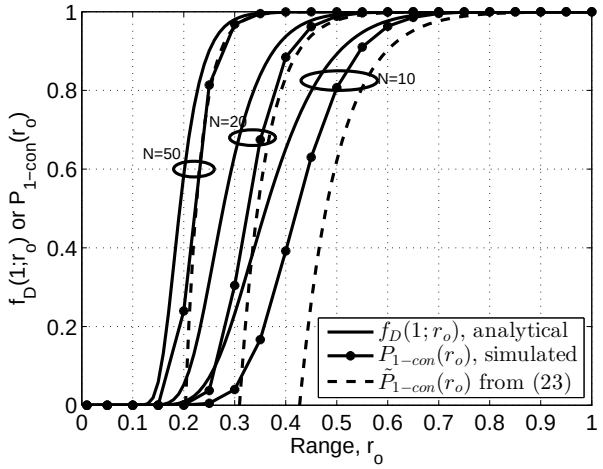

Fig. 11: Probability of connectivity: Upper bound as minimum node degree distribution, $f_D(k; r_{\rm o})$, high density approximation $\tilde{P}_{\text{1-con}}(r_{\rm o})$ and simulated $P_{\text{1-con}}(r_{\rm o})$, versus transmission range $r_{\rm o}$ for $N = 10, 20, 50$ nodes independently and uniformly distributed in a unit square.

D. Network Design Example: Minimum Transmission Range and Minimum Number of Nodes

We now address the network design problems: a) Determine the minimum transmission range r_0^c for given number of nodes or b) Find are the minimum number of nodes N^c, each with given transmission range $r_{\rm o}$, such that the network is k-connected with high probability $P_{\text{k-con}}(r_{\rm o})$, say 0.95 or 0.99. Such a minimum value transmission range and the minimum number of nodes to achieve the desired level of $P_{\text{k-con}}(r_{\rm o})$ are often termed as critical transmission range and critical number of nodes respectively [9], [12], [31]. For a given transmission range, the minimum number of nodes must be deployed to minimize the cost and reduce the interference between the nodes [12]. For a network with fixed number of nodes, the transmission range must be large enough to ensure the network connectivity but it should be small enough to minimize the power consumption and reduce the interference between the nodes.

Since $P_{\text{k-con}}(r_{\rm o})$ is a monotonic function of both transmission range $r_{\rm o}$ and the number of nodes N, the solution to the above problem is to determine the curve in N-$r_{\rm o}$ plane for which $P_{\text{k-con}}(r_{\rm o}) = 0.95$ or $P_{\text{k-con}}(r_{\rm o}) = 0.99$. We can carry out simulations to determine $r_{\rm o}^c$ or N^c. However, as highlighted earlier, it would be very computationally intensive to obtain simulation results with sufficient accuracy, especially for large values of k. We demonstrate here that we can obtain analytical solutions to the design problems mentioned above using the proposed framework. Recalling that minimum node degree distribution $f_D(k; r_{\rm o})$ serves as a good approximation for $P_{\text{k-con}}(r_{\rm o})$, we can use $f_D(k; r_{\rm o})$ given in (20) to determine the critical transmission range and critical number of nodes. The surface plot for $f_D(1; r_{\rm o})$ is shown in Fig. 13 as a function of the number of nodes N and the transmission range $r_{\rm o}$, where we have also shown the analytical curves consisting of $(N, r_{\rm o})$ pairs for which $f_D(1; r_{\rm o}) = 0.95$ or $f_D(1; r_{\rm o}) = 0.99$ and the simulation curves denoting $(N^c, r_{\rm o}^c)$ pairs for which $P_{\text{1-con}}(r_{\rm o}) = 0.95$ or $P_{\text{1-con}}(r_{\rm o}) = 0.99$ with the tolerance of $\pm 0.5\%$. It can be observed that the analytical determination of $(N^c, r_{\rm o}^c)$ using the proposed minimum node degree distribution $f_D(1; r_{\rm o})$ yields a fairly good approximation for both $P_{\text{1-con}}(r_{\rm o}) = 0.95$ and $P_{\text{1-con}}(r_{\rm o}) = 0.99$. Nevertheless, by virtue of our analysis in the previous section and Penrose theorem on connectivity of random graphs [15], the analytical determination is more accurate for $P_{\text{1-con}}(r_{\rm o}) = 0.99$.

VI. Conclusions

In this paper, we have presented a tractable analytical framework for the exact calculation of the probability of node isolation and the minimum node degree distribution in finite wireless sensor networks. We have considered N sensor nodes, each with transmission range $r_{\rm o}$, which are independently and uniformly distributed in a square region. The proposed framework can accurately account for the boundary effects by partitioning the square into subregions, based on the transmission range and the node location. The exact modeling of the boundary effects has not been taken into consideration in previous studies in the literature. Our results confirm that the boundary effects play a key role in determining the connectivity metrics of the network: probability of node isolation, minimum node degree distribution and probability of

This article has been accepted for publication in a future issue of this journal, but has not been fully edited. Content may change prior to final publication. Citation information: DOI 10.1109/TVT.2013.2293580, IEEE Transactions on Vehicular Technology

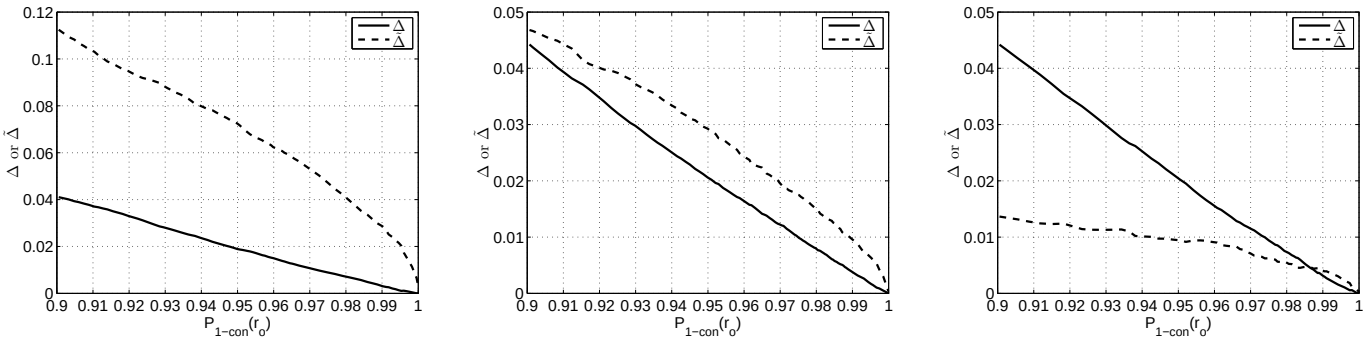

(a) $N = 10$ (b) $N = 20$ (c) $N = 50$

Fig. 12: The differences $\Delta = |P_{\text{1-con}}(r_{\text{o}}) - f_D(1; r_{\text{o}})|$ and $\tilde{\Delta} = |P_{\text{1-con}}(r_{\text{o}}) - \tilde{P}_{\text{1-con}}(r_{\text{o}})|$ denotes the deviation of simulated $P_{\text{1-con}}(r_{\text{o}})$ from the proposed bound as minimum node degree distribution $f_D(1; r_{\text{o}})$ in (20) and high density approximation $\tilde{P}_{\text{1-con}}(r_{\text{o}})$ given in (23) respectively. Both Δ and $\tilde{\Delta}$ are plotted for (a) $N = 10$, (b) $N = 20$ and (c) $N = 50$.

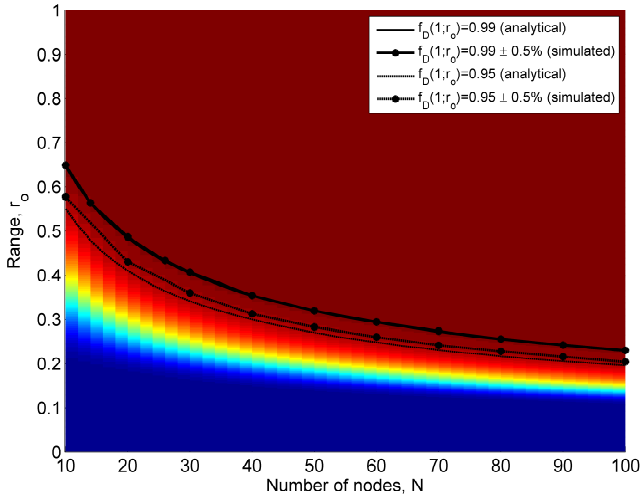

Fig. 13: Surface plot for $f_D(1; r_{\text{o}})$ as a function of number of nodes N and transmission range r_{o}. The curves denote (N, r_{o}) pairs for which $f_D(1; r_{\text{o}}) = 0.95$, or 0.99 and (N^c, r_{o}^c) pairs for which $P_{\text{k-con}}(r_{\text{o}}) = 0.95 \pm 0.5\%$ or $0.99 \pm 0.5\%$.

k-connectivity, especially when the number of nodes is small ($N < 50$). We have also validated the proposed framework with the help of simulations.

Future research can consider natural generalizations of the work presented here. Firstly, the proposed framework can be extended for the case of polygon region (generalization of square region). Secondly, the consideration of the channel fading and interference in the transmission model (generalization of disk model) is an open problem which is outside the scope of this work.

APPENDIX A
MINIMUM NODE DEGREE DISTRIBUTION

Here, we present the formulation of the probability distribution of the minimum node degree D presented in (5). For N uniformly distributed nodes, the number of neighbors d for a node located at $\boldsymbol{u}$ follows a binomial distribution [12], [14], [24]

$$\binom{N-1}{d} \left(F(\boldsymbol{u}; r_{\text{o}})\right)^d \left(1 - F(\boldsymbol{u}; r_{\text{o}})\right)^{N-d-1}$$

and the probability that *any* node in the network has at least d neighbors is therefore given by

$$\binom{N-1}{d} \int_{\mathcal{R}} \left(F(\boldsymbol{u}; r_{\text{o}})\right)^d \left(1 - F(\boldsymbol{u}; r_{\text{o}})\right)^{N-d-1} ds(\boldsymbol{u}).$$

Now the probability that any node in the network has at least k neighbors can be expressed as

$$1 - \sum_{d=0}^{k-1} \binom{N-1}{d} \int_{\mathcal{R}} \left(F(\boldsymbol{u}; r_{\text{o}})\right)^d \left(1 - F(\boldsymbol{u}; r_{\text{o}})\right)^{N-d-1} ds(\boldsymbol{u}),$$

which gives rise to the minimum node degree distribution $f_D(k; r_{\text{o}}) = \text{P}(D = k)$ that all the nodes have at least k neighbors, with an assumption of independence between the nodes. This leads to the result in (5).

REFERENCES

[1] P. Gupta and P. R. Kumar, "Internet in the sky: The capacity of three dimensional wireless networks," *Comm. in Information and Systems*, vol. 1, pp. 33–49, 2001.

[2] X. Hong, M. Gerla, H. Wang, and L. Clare, "Load balanced, energy-aware communications for mars sensor networks," in *Proc. IEEE Aerospace Conference*, vol. 3, 2002.

[3] D. Puccinelli and M. Haenggi, "Wireless sensor networks: applications and challenges of ubiquitous sensing," *IEEE Circuits and Systems Magazine*, vol. 5, no. 3, pp. 19–31, 2005.

[4] J.-H. Cui, J. Kong, M. Gerla, and S. Zhou, "The challenges of building mobile underwater wireless networks for aquatic applications," *IEEE Network*, vol. 20, no. 3, pp. 12–18, May-June 2006.

[5] F. Li and Y. Wang, "Routing in vehicular ad hoc networks: A survey," *IEEE Vehicular Technology Magazine*, vol. 2, no. 2, pp. 12–22, 2007.

[6] P. Fan, G. Li, K. Cai, and K. Letaief, "On the geometrical characteristic of wireless ad-hoc networks and its application in network performance analysis," *IEEE Trans. Wireless Commun.*, vol. 6, no. 4, pp. 1256–1265, Apr. 2007.

[7] F. Fabbri, C. Buratti, and R. Verdone, "A multi-sink multi-hop wireless sensor network over a square region: Connectivity and energy consumption issues," in *Proc. IEEE GLOBECOM*, 2008, pp. 1–6.

[8] J. G. Andrews, R. K. Ganti, M. Haenggi, N. Jindal, and S. Weber, "A primer on spatial modeling and analysis in wireless networks," *IEEE Commun. Mag.*, vol. 48, no. 11, pp. 156–163, Nov. 2010.

[9] P.-J. Wan, C.-W. Yi, and L. Wang, "Asymptotic critical transmission radius for k-connectivity in wireless ad hoc networks," *IEEE Trans. Inf. Theory*, vol. 56, no. 6, pp. 2867–2874, 2010.

[10] G. Mao, "Research on wireless multi-hop networks: Current state and challenges," in *Proc. ICCNC*, 2012.

[11] F. Baccelli and B. Blaszczyszyn, *Stochastic geometry and wireless networks, volume 1 & 2: Theory and applications*. Foundations and Trends in Networking, 2009.

[12] C. Bettstetter, "On the minimum node degree and connectivity of a wireless multihop network," *Proc. 3rd ACM International Symposium on Mobile Ad Hoc Networking & Computing*, vol. 9, no. 11, pp. 80–91, 2002.

[13] Z. Khalid and S. Durrani, "Connectivity of three dimensional wireless sensor networks using geometrical probability," in *Proc. Australian Communications Theory Workshop (AusCTW)*, 2013, pp. 47–51.

[14] C. Bettstetter, "On the connectivity of ad hoc networks," *The Computer Journal*, vol. 47, no. 4, pp. 432–447, 2004.

[15] M. Penrose, "The longest edge of the random minimal spanning tree," *The Annals of Applied Probability*, vol. 7, no. 2, pp. 340–361, 1997.

[16] P. Gupta and P. Kumar, "Critical power for asymptotic connectivity in wireless networks," in *Proc. IEEE CDC*, vol. 1, 1998, pp. 1106–1110.

[17] Q. Ling and Z. Tian, "Minimum node degree and k-connectivity of a wireless multihop network in bounded area," in *Proc. IEEE GLOBECOM*, 2007, pp. 1296–1301.

[18] D. Miorandi, E. Altman, and G. Alfano, "The impact of channel randomness on coverage and connectivity of ad hoc and sensor networks," *IEEE Trans. Wireless Commun.*, vol. 7, no. 3, pp. 1062–1072, Mar. 2008.

[19] X. Zhou, H. Jones, S. Durrani, and A. Scott, "Effect of beamforming on the connectivity of ad hoc networks," in *Proc. Australian Communications Theory Workshop (AusCTW)*, 2007, pp. 13–18.

[20] X. Zhou, S. Durrani, and H. M. Jones, "Connectivity analysis of wireless ad hoc networks with beamforming," *IEEE Trans. Veh. Technol.*, vol. 58, no. 9, pp. 5247–5257, Nov. 2009.

[21] S. C. Ng, G. Mao, and B. D. O. Anderson, "Critical density for connectivity in 2D and 3D wireless multi-hop networks," *IEEE Trans. Wireless Commun.*, vol. 12, no. 4, pp. 1512–1523, 2013.

[22] W. Jia and J. Wang, "Analysis of connectivity for sensor networks using geometrical probability," *IEE Proceedings Communications*, vol. 153, no. 2, pp. 305–312, Apr. 2006.

[23] F. Fabbri and R. Verdone, "A statistical model for the connectivity of nodes in a multi-sink wireless sensor network over a bounded region," in *Proc. 14th European Wireless Conference*, June 2008.

[24] S. Srinivasa and M. Haenggi, "Distance distributions in finite uniformly random networks: Theory and applications," *IEEE Trans. Veh. Technol.*, vol. 59, no. 2, pp. 940–949, Feb. 2010.

[25] A. Eslami, M. Nekoui, H. Pishro-Nik, and F. Fekri, "Results on finite wireless sensor networks: Connectivity and coverage," *ACM Trans. Sen. Netw.*, vol. 9, no. 4, pp. 51:1–51:22, Jul. 2013.

[26] G. Mao and B. D. O. Anderson, "Towards a better understanding of large-scale network models," *IEEE/ACM Transactions on Networking*, vol. 20, no. 2, pp. 408–421, Apr. 2012.

[27] J. P. Coon, C. P. Dettmann, and O. Georgiou, "Full connectivity: Corners, edges and faces," *J. Stat. Phys.*, vol. 147, pp. 758–778, 2012.

[28] A. M. Mathai, *An introduction to geometrical probability: Distributional aspects with applications*. CRC Press, 1999.

[29] G.-C. Aboue Nze, F. Guinand, and Y. Pigne, "Impact of square environment on the connectivity in finite ad hoc networks," in *Proc. 14th International Symposium on Wireless Personal Multimedia Communications (WPMC)*, 2011.

[30] R. Rajagopalan and P. Varshney, "Connectivity analysis of wireless sensor networks with regular topologies in the presence of channel fading," *IEEE Trans. Wireless Commun.*, vol. 8, no. 7, pp. 3475–3483, Jul. 2009.

[31] P.-J. Wan and C.-W. Yi, "Asymptotic critical transmission ranges for connectivity in wireless ad hoc networks with bernoulli nodes," in *Proc. IEEE Wireless Communications and Networking Conference, 2005*, vol. 4, 2005, pp. 2219–2224.

[32] P. Santi, D. M. Blough, and F. Vainstein, "A probabilistic analysis for the range assignment problem in ad hoc networks," in *Proc. 2nd ACM international symposium on Mobile ad hoc networking & computing*. New York, NY, USA: ACM, 2001, pp. 212–220.

[33] Z. Khalid and S. Durrani, "Distance distributions in regular polygons," *IEEE Trans. Veh. Technol.*, vol. 62, no. 5, pp. 2363–2368, Jun. 2013.

[34] U. Bäsel, "Random chords and point distances in regular polygons," *ArXiv Technical Report*, 2012. [Online]. Available: http://arxiv.org/abs/1204.2707

[35] M. K. Simon and M.-S. Alouini, *Digital Communication over fading channels*, 2nd ed. Wiley, 2005.

[36] G.-C. Nze and F. Guinand, "Mean degree of ad hoc networks in environments with obstacles," in *Proc. IEEE 8th International Conference on Wireless and Mobile Computing, Networking and Communications (WiMob)*, 2012, pp. 381–388.

Zubair Khalid (S'10-M'13) received his B.Sc. (first-class hons.) degree in Electrical Engineering from the University of Engineering & Technology (UET), Lahore, Pakistan in 2008. He received the Ph.D. degree in Engineering from the Australian National University of Canberra, Australia in Aug. 2013. He is currently working as Research Fellow in Research School of Engineering, the Australian National University (ANU), Canberra, Australia. Zubair was awarded University Gold Medal and Industry Gold Medals from Siemens and Nespak for his overall outstanding performance in Electrical Engineering during the his undergraduate studies. He was a recipient of an Endeavour International Postgraduate Award for his Ph.D. studies. He was also awarded an Dean's Travel Grant in 2012 and ANU Vice Chancellor's Higher Degree Research travel grant in 2011. His research interests are in the area of signal processing and wireless communications, including the development of novel signal processing techniques for signals on the sphere and application of stochastic geometry in wireless ad-hoc networks .

Salman Durrani (S'00-M'05-SM'10) received the B.Sc. (1st class honours) degree in Electrical Engineering from the University of Engineering & Technology, Lahore, Pakistan in 2000. He received the PhD degree in Electrical Engineering from the University of Queensland, Brisbane, Australia in Dec. 2004. He has been with the Australian National University, Canberra, Australia, since 2005, where he is currently Senior Lecturer in the Research School of Engineering, ANU College of Engineering & Computer Science. His current research interests are in wireless communications and signal processing, including synchronization in communication systems, outage and connectivity of wireless energy harvesting systems and ad-hoc networks and signal processing on the unit sphere. He has co-authored more than 65 publications to date in refereed international journals and conferences. He is a Member of Engineers Australia and a Senior Fellow of The Higher Education Academy, UK.

Jing Guo (S'12) received her BSc (first class honours) in electronics and telecommunications engineering from the Australian National University, Australia and the Beijing Institute of Technology, China in 2012. She is currently pursuing the PhD degree at the Research School of Engineering, Australian National University, Canberra, Australia. She is a recipient of an ANU International PhD scholarship for the duration of her PhD degree. She was awarded an ANU University medal for her outstanding academic performance during her undergraduate studies. Her research interest lies in the field of wireless communications and includes the application of stochastic geometry in wireless networks.